Monthly means of reflected solar flux from POLDER (ADEOS-1) and comparison with ERBE, ScaRaB and CERES

Michel Viollier, Carsten Standfuss, Frédéric Parol

Monthly means of reflected solar flux from POLDER (ADEOS-1) and comparison with ERBE, ScaRaB and CERES

Michel Viollier and Carsten Standfuss[1]

Laboratoire de Météorologie Dynamique, C.N.R.S., Ecole Polytechnique, Palaiseau, France

Frédéric Parol

Laboratoire d'Optique Atmosphérique, Université des Sciences et Techniques de Lille, Lille, France

Received 25 October 2001; revised 11 March 2002; accepted 14 March 2002; published 31 May 2002.

[1] A diurnal cycle model is applied to POLDER instantaneous albedo determinations (Nov. 1996–June 1997) in order to compute daily and monthly means of the reflected flux at the top of the atmosphere. These results are compared to the ERBE, ScaRaB and CERES records. The quantitative comparison of the tropical means shows that the POLDER reflected flux density is on average lower by about 7 Wm^{-2} compared to ERBE (1985–1989) and ScaRaB-1 (1994–1995) and by 2.7 Wm^{-2} compared to ScaRaB-2 (Nov. 1998–March 1999) and CERES/Terra (2000–). The maps of POLDER albedo reveal strong deviations in the tropical Pacific. They correspond to the beginning of the 1997–1998 ENSO event. *INDEX TERMS:* 3309 Meteorology and Atmospheric Dynamics: Climatology (1620); 3394 Meteorology and Atmospheric Dynamics: Instruments and techniques; 1610 Global Change: Atmosphere (0315, 0325); 1694 Global Change: Instruments and techniques; 3360 Meteorology and Atmospheric Dynamics: Remote sensing

1. Introduction

[2] On board ADEOS-1, the 'Polarization and Directionality of Earth's Reflectance' (POLDER) instrument provided global and repetitive observations of the Earth from November 1996 to June 1997. With a new instrumental concept (multi-spectral radiometer and polarimeter with multi-angle observation ability, *Deschamps et al.* [1994] POLDER has demonstrated new methods of remote sensing in different fields (cloud and aerosol properties, land surface characteristics, ocean color). POLDER is also expected to contribute to the determination of the Earth Radiation Budget (ERB) by improving the estimate of the reflected shortwave (SW) radiation. Thanks to its multi-angle observations, POLDER obtains direct information on the anisotropy of the reflected radiation field. However, due to the lack of a broadband solar channel and of in-flight calibration facilities, POLDER is not an ERB-dedicated instrument like ERBE [*Barkstrom et al.*, 1989], ScaRaB [*Kandel et al.*, 1998, *Duvel et al.*, 2001] or CERES [*Wielicki et al.*, 2002]. On the other hand it may contribute to the long-term ERB observation record. The instantaneous broadband or shortwave albedo A_{SW} is already operationally derived as a function of narrow-band albedos at 443, 670 and 865 nm [*Buriez et al.*, 1997]. This instantaneous albedo at the local time of the observation (around 10:30 am) can be found in the level-2 product of the POLDER 'ERB and clouds' line. However, the instantaneous albedo is not equivalent to the daily average. They would be equivalent only if the changes in cloudiness during the day could be ignored and if the albedo of a constant scene did not vary with solar zenith angle. This is not the case: for a constant scene the daily averaged albedo is generally higher than the 10:30 instantaneous albedo, typically by 15%. There is however no simple relationship between them. For this reason, diurnal interpolation and extrapolation procedures (DIEP) have been developed for ERBE [*Brooks et al.*, 1986] and for ScaRaB [*Standfuss et al.*, 2001]. In this paper we have adjusted these algorithms to POLDER in order to compute daily and monthly means of the SW reflected flux density and to compare with ERBE, ScaRaB and CERES determinations.

2. Description of the Input Data: Instantaneous Albedos

[3] The SW instantaneous albedos are estimated from the measured radiances using empirical or theoretical models of the anisotropy of the reflected radiation field. The ERBE-type algorithms of ScaRaB and CERES use an empirical angular model based on a 12-scene-type-classification [*Suttles et al.*, 1988]. The POLDER case is far different. First, spectral albedos at 443, 670 and 865 nm are estimated from the corresponding radiances by using a plane parallel model; then, the SW albedo is derived from the spectral albedos based on radiative transfer calculations accounting for atmospheric scattering and for ozone and water vapor absorption [*Buriez et al.*, 1997]. This theoretical approach could be a source of error and needs further study. Spatial and temporal characteristics of these experiments also differ. In ERBE, scanner data from sun-synchronous satellites (NOAA 9 and 10) were combined with the ERBS precessing (72 days) satellite. The first CERES instrument flew on the TRMM precessing (46 days) satellite. ScaraB-1 was on Meteor 3–7 with a 213-day precession period so that observation time was slowly drifting. On the contrary, POLDER, ScaRaB-2 and CERES/Terra are all on sun-synchronous satellites with similar equatorial crossing time, around 10:30 local time: comparisons between these last 3 data-sets will not be affected by the time sampling characteristics. The footprint of ERB instruments are a few tens of kilometers (about 40 km at nadir for ScaRaB-2) and the flux is averaged over areas of 2.5° by 2.5° in longitude and latitude to perform the ERBE-type processing of regional and monthly means. The POLDER footprint is approximately 6 km and the level-2 parameters are averaged over typically 9×9 (3×3 in future version) to form a 'superpixel' of 0.5° by 0.5° at the equator. The diurnal extrapolation procedures explained in the next section have been applied to the 2.5° regional averages of ScaRaB and CERES and to the 0.5° POLDER averages.

3. Description of the Diurnal Extrapolation Procedures

[4] The purpose of the SW diurnal model is to extrapolate the instantaneous albedo α from observation time t_{obs} to the 24 local

[1]Now at NOVELTIS, Ramonville-St Agne, France.

0094-8276/02/2001GL014255

Table 1. Scene Identification Using POLDER Level 2 Parameters (c.s. = clear sky, p.c. = partly cloudy, m.c. = mostly cloudy, o. = overcast)

	Scene type	Geotype	Cloud Cover	Cloud Optical Thickness
1	c. s. ocean	ocean	[0.0, 0.05[	-
2	c. s. land	land		
3	c. s. coast	coast		
4	c. s. desert, north hm	desert		
5	c. s. desert, south hm	desert		
6	ice / snow	any	[0.0, 0.95]	any
7	p.c. ocean	ocean	[0.05, 0.5[	
8	p.c. land	land or desert		
9	p.c. coast	coast		
10	m.c. ocean	ocean	[0.5, 0.95]	
11	m.c. land	land or desert		
12	m.c. coast	coast		
13	o. very thick, liquid	any	]0.95, 1.0]	[20 , ∞[
14	o. very thick, non-l.			
15	o. thick, ocean	ocean or coast		[10, 20[
16	o. thick, land	land or desert		
17	o. thin, ocean	ocean or coast		[4, 10[
18	o. thin, land	land or desert		
19	o. very thin, ocean	ocean or coast		[0, 4[
20	o. very thin, land	land or desert		

hour boxes centered on the local half hour t_h: 0030, 0130, ..., 2330. Assuming that the observed scene is constant throughout the day, equation (1) takes into account the predictable variation of the solar zenith angle θ_0 and its influence on the albedo through the scene type dependent directional function α_j^{dir}

$$\alpha(t_h) = \sum_j f_j(t_{obs})\alpha_j(t_{obs})\frac{\alpha_j^{dir}(\theta_0(t_h))}{\alpha_j^{dir}(\theta_o(t_{obs}))} \quad (1)$$

In the ERBE algorithms (see *Brooks et al.*, 1986), this equation is applied for the four cloud cover ranges according to the fraction f_j of scene types j present in the considered 2.5° region, using the directional albedos α_j^{dir} provided by *Suttles et al.* [1988] and the observed albedo α_j per scene type. If at least two SW observations are available, two series of extrapolated flux estimations are computed, and the flux is linearly interpolated between the two observation hours. For each region, the daily and the monthly means of the diurnal albedos are then computed as well as the corresponding reflected flux density (Wm^{-2}) at the top of the atmosphere.

[5] The ERBE scene identification is based on the analysis of both SW and infrared radiances and thus cannot be applied to POLDER. However, the multi-spectral, multi-directional and polarization analyses of POLDER provide a better description of cloud parameters [*Parol et al.*, 1999]. In order to benefit from this, a scene identification based on 20 types has been introduced. This new scene classification distinguishes four ranges of cloud fraction (clear sky < 5%, partly cloudy 5–50%, mostly cloudy 50–95%, and overcast > 95%) using the POLDER cloud cover, four intervals of cloud optical thickness at 670 nm and the cloud phase. The surface type (ocean, land, snow/ice, desert, land-ocean mix) is determined using the POLDER scene indicator. Details are shown in Table 1. Based on 4 months of POLDER data (Nov 1996, Feb 1997, May 1997 and June 1997), for each of these 20 scene types, the directional albedo functions have been calculated by averaging the POLDER albedos in solar angle bins (0.02 of width in cos θ_0) and by fitting the results with a third-order polynomial function of cos θ_0 to smooth for latitudinal variations of scene type occurences.

For desert scenes where the solar zenith angle sampling is too limited, the directional models of *Capderou* [1998] are adopted. It has been quantified that the sensitivity of regional monthly means on the use of POLDER or ERBE models is below 4 Wm^{-2} and 1 Wm^{-2} for rms and bias respectively. With these directional albedo functions, equation 1 is applied to extrapolate the 10:30 albedo to the other hours of the day.

[6] Except when several observations are available in the day, the ERBE-type method is based on the assumption of diurnally constant cloud conditions. *Standfuss et al.* [2001] have improved this approach by introducing adjustments based on a regional diurnal albedo climatology computed from the 5 years of ERBS scanner data (1985–1990). The new method uses the hourly climatological albedo instead of the ERBE directional albedo to extrapolate the SW flux from the observation to each local hour independently of the scene type. Equation 1 is replaced by

$$\alpha(t_h) = \alpha(t_{obs})\frac{\alpha^{cli}(t_h)}{\alpha^{cli}(t_{obs})} \quad (2)$$

where α^{cli} is the monthly climatological albedo defined for each 2.5° × 2.5° ERBE region and for each local hour. The climatological albedo implicitly accounts for the θ_0-dependent directional variations and the time-dependent meteorological variations. However, the extrapolation with equation 2 may lead to unrealistic values when the observed albedo deviates strongly from the 'climatological' albedo (e.g. in case of a climate anomaly). To avoid this problem, appropriate restrictions for the application of equation 2 have been defined. The ERBE-type (equation 1) and the 'climatological' (equation 2) extrapolation are applied concurrently giving $\alpha^E(t)$ and $\alpha^C(t)$. Separately for each hour, the middle value between the ERBE-like albedo $\alpha^E(t)$, the climatologically extrapolated albedo $\alpha^C(t)$ and the climatological mean $\alpha^{Cli}(t)$ is chosen. Typically, the 'climatological' extrapolation is used in 60% of the cases. On the global scale, the regional monthly time sampling error (up to 40 Wm^{-2}) of the ERBE-type extrapolation is reduced by about 20% for single NOAA-AM and PM observations. This is due to a high efficiency of the climatological extrapolation in areas with a coherent diurnal cycle of cloudiness (morning oceanic low cloud and afternoon convection) and a neutral behaviour elsewhere. Both diurnal extrapolation techniques are applied to POLDER data using the 20 POLDER directional albedo models in equation 1. For the zonal and global means, the difference is almost negligible since positive and negative effects of the climatological extrapolation cancel out. On regional scale, the differences between ERBE-type extrapolated and climatologically extrapolated monthly mean flux densities (not shown) are small (± 5 Wm^{-2} typically) as compared to

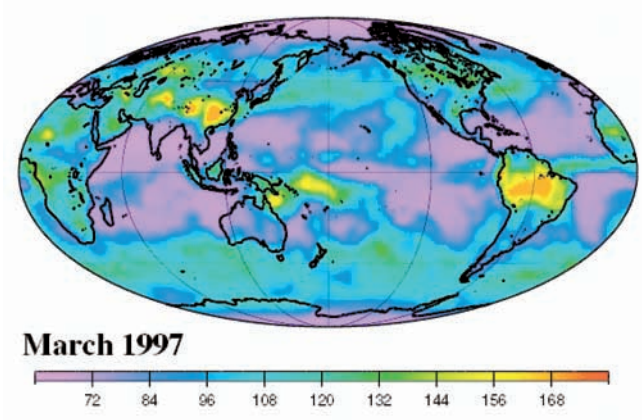

Figure 1. SW reflected flux density (Wm^{-2}) for March 1997 (POLDER/ADEOS).

the magnitude of inter-annual regional anomalies (>20 Wm^{-2}) shown hereafter. The errors due to the narrow-to-broad band conversion and the radiance-to-flux conversion (about 10% for the instantaneous flux estimations) are expected to be reduced to the 2% level by the space and time averaging processes assuming large statistical independence of the error sources. Therefore the monthly mean uncertainty results from these errors in addition to the calibration (4–6%, *Hagolle et al.* [1999]) and time sampling errors. For the tropical monthly means (about 90 Wm^{-2}), discussed hereafter in this paper, the uncertainty may reach more than 7 Wm^{-2}.

4. Results

[7] The eight monthly means of POLDER-1 have been processed at the super pixel scale and averaged into the 2.5° × 2.5° ERBE grid. Monthly regional reflected fluxes are shown on Figure 1 for March 1997, and the anomalies for February, March and July 1997 on Figure 2. Anomalies are departures from the 1985–1989 ERBE monthly means. On Figure 1, low fluxes (in purple) are found in cloud-free oceanic areas and in polar zones. Mid-latitude cloud regimes and the Atlantic ITCZ are characterized by fluxes above the global average (green). The highest fluxes (yellow and red) correspond to cloudy areas in South America and China but also to enhanced tropical convection over the western Pacific whereas large parts of Indonesia are cloud free. This unusual observation is the most important feature of our series. It corresponds to the beginning of the 1997–1998 ENSO warm event and can be better examined on the anomaly maps (Figure 2). The February anomaly map (Figure 2a) shows enhanced tropical convection over Indonesia and eastern Indian Ocean (indicated by positive anomalies of the reflected flux). In March 1997 (Figure 2b), the anomaly pattern shows the suppressed convection (in blue) over Indonesia and the enhanced convection (in red) in the western Pacific. The eastward progress of the convection continues during the following months (June, Figure 2c). All these SW observations fit well the evolution of the 1997 El Niño [*Bell and Halpert*, 1998], specifically the SW anomalies correspond to corresponding (i.e., opposite) anomalies of the outgoing longwave radiation.

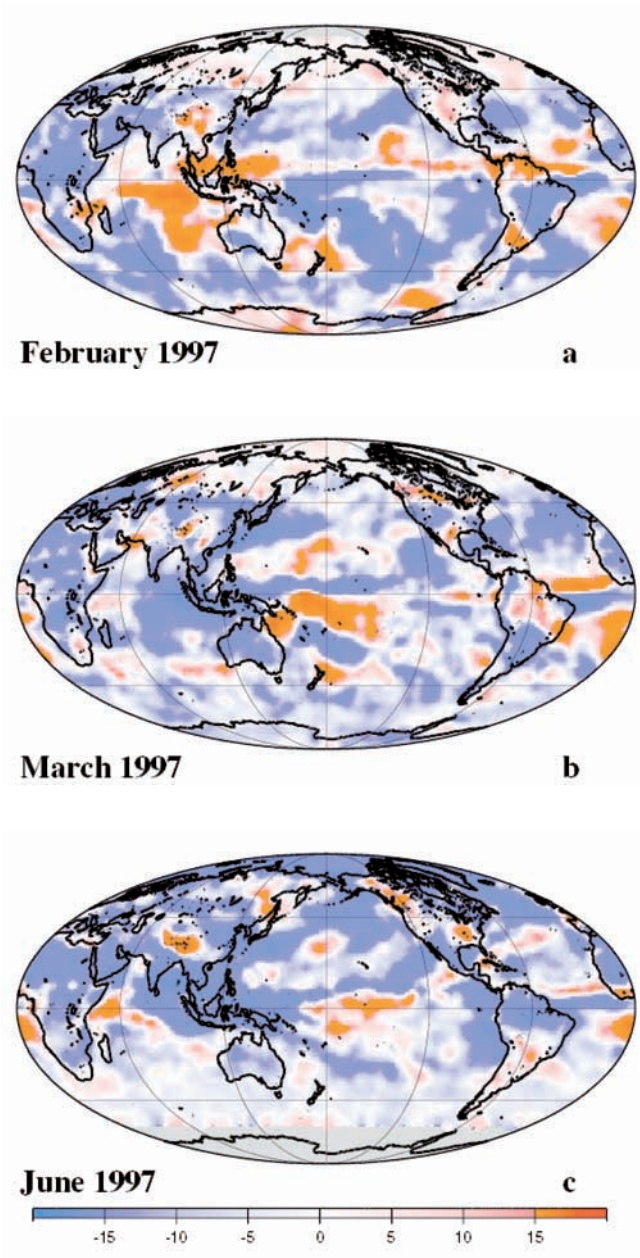

Figure 2. SW reflected flux density anomalies (Wm^{-2}) for (a) February, (b) March, and (c) June 1997, referenced to the 1985–1989 ERBE monthly means.

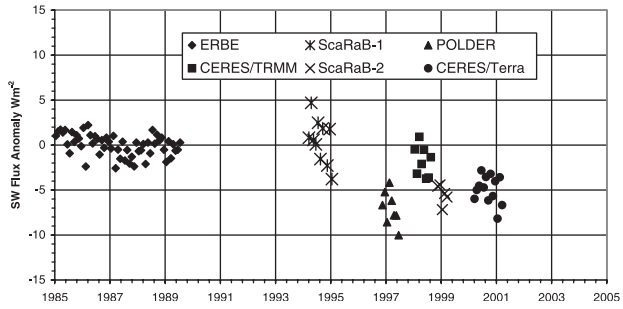

Figure 3. 20S-20N SW flux density anomalies referenced to 1985–1989 monthly means.

[8] The prime color of the anomaly maps (Figure 2) is blue: in average POLDER gives lower albedo than ERBE. To quantify this difference we use the tropical mean. Defined in the CERES program [*Wielicki et al.*, 2002], the tropical mean corresponds to the latitudinal belt between ±20° and is useful to compare various data including data from satellites with low orbit inclination such as CERES/TRMM. Figure 3 shows the monthly anomaly of the SW flux for all ERB missions since ERBE, again referenced to 1985–1989 ERBE monthly means. The ScaRaB-1 means are the most scattered, probably due to the continuous drift of the observation time (February 1995 is not shown since observed in terminator conditions). The most remarkable feature is the bias of about −4 Wm^{-2} observed both for ScaRaB-2 and CERES/Terra (Flight Model 1 and Edition 1). Although instrument analysis errors (generally estimated to 5 Wm^{-2}) cannot be completely excluded to explain a part of the difference, this SW drop may reveal a real decadal change in tropical cloudiness [*Wielicki et al.*, 2002]. Furthermore, POLDER is the darkest in the series: in average −7 Wm^{-2} from ERBE and −2.7 Wm^{-2} from CERES/Terra but within the uncertainty range estimated to about 7 Wm^{-2}.

5. Conclusion

[9] The daily averaged reflected SW flux density has been computed for the 8 months of POLDER-1 on ADEOS, and the monthly means are compared with corresponding estimations from ERB dedicated experiments. In average, the POLDER 20S–20N reflected solar flux density is smaller by about 2.7 Wm^{-2} and

7 Wm^{-2} respectively when compared to CERES/Terra and ERBE for a mean value of about 90 Wm^{-2}. This 3–7% agreement between very different instruments and methodologies (calibration, angular correction) is remarkable and consistent with regard to the 4–6% uncertainties in the POLDER calibration and to the other various error sources. The regional flux distribution exhibits large similarities with the ERB series except in the tropical Pacific where the anomalies are related to the beginning of the 1997–1998 ENSO event, particularly the extremely rapid shift of the enhanced convection easterly from Indonesia to the western Pacific in March 1997. When POLDER/ADEOS-2 is in operation (planned for Nov. 2002), more accurate comparisons can be done with almost simultaneous observations from CERES/Terra. In this context, the error budget of the POLDER albedo retrieval (in particular the narrow-to-broadband conversion) may be consolidated and the advanced multi-angular information from POLDER may be compared with corresponding CERES anisotropy models.

[10] **Acknowledgments.** The CERES data were obtained from NASA (LARC/EOSDIS/DAAC). The POLDER data were provided from CNES and LOA. We thank Jean Claude Buriez and three anonymous reviewers for helpful comments and Patrick Raberanto for his help in data processing.

References

Barkstrom, B. R., et al., Earth Radiation Budget Experiment (ERBE) archival and April 1985 results, *Bull. Amer. Meteor. Soc.*, *70*, 1254–1262, 1989.

Bell, G. D., and M. S. Halpert, Climate Assessment for 1997, *Bull. Amer. Meteor. Soc.*, *79*, S1–S50, 1998.

Brooks, D. R., E. H. Harrison, P. Minnis, J. T. Suttles, and R. Kandel, Development of Algorithms for Understanding the Temporal and Spatial Variability of the Earth's Radiation Balance, *Rev. Geophys.*, *24*, 422–438, 1986.

Buriez, J. C., C. Vanbauce, F. Parol, P. Gouloub, M. Herman, B. Bonnel, Y. Fouquart, P. Couvert, and G. Sèze, Cloud detection and derivation of cloud properties from POLDER, *Int. J. Remote Sensing*, *18*, 2785–2813, 1997.

Capderou, M., Determination of the shortwave anisotropic function for clear-sky desert scenes from ScaRaB data. Comparisons with models issued from other satellite data, *J. Appl. Met.*, *37*, 1398–1411, 1998.

Deschamps, P.-Y., F.-M. Bréon, M. Leroy, A. Podaire, A. Bricaud, J.-C. Buriez, and G. Sèze, The POLDER mission: Instrument characteristics and scientific objectives, *IEEE Trans. on Geoscience and Remote Sensing*, *32*, 598–615, 1994.

Duvel, J. P., et al., The ScaRaB-Resurs Earth Radiation Budget Dataset and first results, *Bull. Amer. Meteor. Soc.*, *82*, 1397–1408, 2001.

Hagolle, O., P. Goloub, P. Y. Deschamps, H. Cosnefroy, X. Briottet, T. Bailleul, J. M. Nicolas, F. Parol, B. Lafrance, and M. Herman, Results of POLDER in-flight calibration, *IEEE Trans. on Geoscience and Remote Sensing*, *37*, 1550–1566, 1999.

Kandel, R., et al., The ScaRaB Earth Radiation Budget Dataset, *Bull. Amer. Meteor. Soc.*, *79*, 765–783, 1998.

Parol, F., J.-C. Buriez, C. Vanbauce, P. Couvert, G. Sèze, P. Gouloub, and S. Cheinet, First results of the POLDER "Earth Radiation Budget and Clouds" operational algorithm, *IEEE Trans. on Geoscience and Remote Sensing*, *37*, 1597–1612, 1999.

Standfuss, C., M. Viollier, R. S. Kandel, and J. Ph. Duvel, Regional Diurnal Albedo Climatology and Diurnal Time Extrapolation of Reflected Solar Flux Observations, Application to the ScaRaB record, *J. Climate*, *14*, 1129–1146, 2001.

Suttles, J. T., R. N. Green, P. Minnis, G. L. Smith, W. F. Staylor, B. A. Wielicki, I. J. Walker, D. F. Young, V. R. Taylor, and L. L. Stowe, Angular radiation models for Earth-atmosphere system. Volume I—Shortwave radiation, *NASA reference publication*, *1184*. 144 pp., 1988.

Wielicki, B. A., T. Wong, R. P. Allan, A. Slingo, J. T. Kiehl, B. J. Soden, C. T. Gordon, A. J. Miller, S.-K. Yang, D. A. Randall, F. Robertson, J. Susskind, and H. Jacobowitz, Evidence for Large Decadal Variability in the Tropical Mean Radiative Energy Budget, *Science*, *295*, 841–844, 2002.

M. Viollier, Laboratoire de Météorologie Dynamique, C.N.R.S., Ecole Polytechnique, 91128 Palaiseau Cedex, France. (viollier@lmd.polytechnique.fr)

C. Standfuss, NOVELTIS, Parc Technologique du Canal, 2 Avenue de l'Europe, 31520 Ramonville-St Agne, France. (carsten.standfuss@noveltis.fr)

F. Parol, Laboratoire d'Optique Atmosphérique, Université des Sciences et Techniques de Lille, 59655 Villeneuve d'Ascq Cedex, France. (Frederic.Parol@univ-lille1.fr)